

Article

Heterogeneous Fenton Oxidation with Natural Clay for Textile Levafix Dark Blue Dye Removal from Aqueous Effluent

Manasik M. Nour¹, Maha A. Tony^{2,3} and Hossam A. Nabwey^{1,2,*} 

¹ Department of Mathematics, College of Science and Humanities in Al-Kharj, Prince Sattam Bin Abdulaziz University, Al-Kharj 11942, Saudi Arabia; h.mohamed@psau.edu.sa

² Basic Engineering Science Department, Faculty of Engineering, Menoufia University, Shebin El-Kom 32511, Egypt; dr.maha.tony@gmail.com

³ Advanced Materials/Solar Energy and Environmental Sustainability (AMSEES) Laboratory, Faculty of Engineering, Menoufia University, Shebin El-Kom 32511, Egypt

* Correspondence: eng_hossam21@yahoo.com

Abstract: The ever-increasing technological advancement and industrialization are leading to a massive discharge of hazardous waste into the aquatic environment, calling on scientists and researchers to introduce environmentally benign solutions. In this regard, the current work is based on introducing Fuller's earth, which is regarded as an environmentally benign material, as an innovative Fenton oxidation technology to treat effluent loaded with Levafix Dark Blue dye. Initially, Fuller's earth was chemically and thermally activated, then subjected to characterization using a field-emission scanning electron microscope (FE-SEM) augmented with an energy-dispersive X-ray analyzer (EDX) and Fourier transform infrared (FTIR). This detailed the morphologies of the samples and the functional groups on the catalyst leading to the reaction with the dye. Fuller's earth, augmented with hydrogen peroxide, was then introduced as a photo-Fenton oxidation system under UV illumination for dye oxidation. Moreover, a response surface mythological analysis was applied to optimize the most effective operational parameters. The experimental data revealed that the optimal Fuller's earth dose corresponded to 1.02 mg/L using the optimal H₂O₂ of 818 mg/L at pH 3.0, and the removal efficiency reached 99%. Moreover, the thermodynamic parameters were investigated, and the data revealed the positive $\Delta G'$ and negative $\Delta S'$ values that reflect the non-spontaneous nature of oxidation at high temperatures. Additionally, the negative $\Delta H'$ values suggest the occurrence of the endothermic oxidation reaction. Furthermore, the reaction followed the second-order kinetic model. Finally, the catalyst stability was investigated, and reasonable removal efficiency was attained (73%) after the successive use of Fuller's earth reached six cyclic uses.

Keywords: wastewater; clay; Fuller's earth; Levafix Dark Blue dye; oxidation; Fenton



Citation: Nour, M.M.; Tony, M.A.; Nabwey, H.A. Heterogeneous Fenton Oxidation with Natural Clay for Textile Levafix Dark Blue Dye Removal from Aqueous Effluent. *Appl. Sci.* **2023**, *13*, 8948. <https://doi.org/10.3390/app13158948>

Academic Editors: Dae Sung Lee, Yolanda Patiño and Amanda Laca Pérez

Received: 19 May 2023

Revised: 21 July 2023

Accepted: 26 July 2023

Published: 3 August 2023



Copyright: © 2023 by the authors. Licensee MDPI, Basel, Switzerland. This article is an open access article distributed under the terms and conditions of the Creative Commons Attribution (CC BY) license (<https://creativecommons.org/licenses/by/4.0/>).

1. Introduction

Currently, since a greener environment is the hallmark of the scientific world, the contribution of naturally abundant clay minerals is notably visible. In recent decades, clay minerals based on Fuller's earth [1] have been used to modify the performance of photocatalytic reactions. Scientists are inspired by the outstanding characteristics of clay since it is abundant, cost-efficient, and benign to the environment and ecosystem [2]. Although Fuller's earth was first discovered in 1847, clay science is associated with prehistoric times. Its use in several applications can be traced back to 200 cultures, such as the ancient Egyptians, Amargosians, and South and North Americans [3,4]. Recently, Fuller's earth-based semiconductors have attracted great attention for their efficient performance in photocatalytic reactions for eliminating various contaminants from wastewater streams.

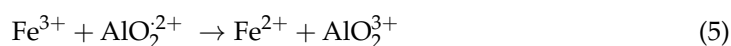
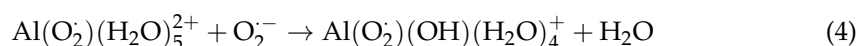
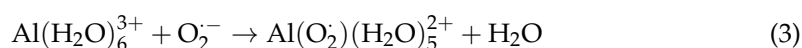
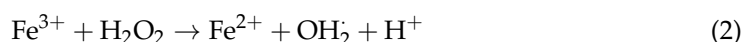
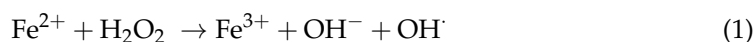
However, with the ever-increasing development of societies and the global industrialization revolution, the problems associated with environmental pollution are also tremendously increasing [5]. Massive amounts of organic dyes are discharged annually

from various industries. Such industries include the printing and paper industry, photographic industries, tanning and leather industries, and textile dyeing industries [6]. The textile industry is considered the most polluting industry in the industrial sector [6]. This industry consumes substantial amounts of water in its processing and finishing. Thus, the result is a huge amount of wastewater contaminated with various dye species. Such waste causes persistent damage to the environment [7]. Most of the dyes included in this aqueous effluent are carcinogenic and cause severe damage to the ecosystem and its inhabitants. Hence, such contaminated wastewater must undergo treatment prior to its final disposal into the environment. When comparing photocatalytic reactions to other wastewater treatment technologies, the photocatalytic system is a superior candidate. This might be due to its complete mineralization tendency for contaminants in aqueous streams [8]. Among the photocatalytic reactions, the iron-based catalytic reaction that uses Fe^{2+} and Fe^{3+} as typical iron sources, the so-called Fenton reaction, has attracted scientists' attention for its unique photocatalytic activity [9]. Moreover, its use in contaminate elimination has increased due to the reaction being cost-efficient and the catalyst possessing optical properties [10]. Although the properties of this reaction are superior, there are three main defects that restrict its application. The obstructions are the chemical precursor's price, the need for an acidic pH medium for treatment, and the byproduct sludge after treatment that requires further handling prior to the final discharge [11]. From this concept, various trials have been developed to overcome these drawbacks of the Fenton process. For instance, introducing hetero-junction catalytic materials as the precursors of the Fenton reaction is an excellent strategy due to both its superior catalytic advances and its recovery ability [12]. Moreover, replacing Fe^{2+} or Fe^{3+} with non-iron metals, such as Cu^{2+} , shows excellent results since this widens the acidic pH range. Furthermore, aluminum has been shown to be an excellent replacement for Fe^{2+} or Fe^{3+} in the reagent as a non-iron Fenton system [13]. Moreover, the aluminum that is present in natural-based materials [14] might be applied to initiate the iron-based Fenton system as a non-iron system [15].

Scientists' crucial goal is identifying environmentally benign materials. In this regard, the naturally abundant Fuller's earth is a suitable candidate. Fuller's earth is the main component of clay minerals that comprise silicon, calcium, and aluminum oxides with a dominant fraction of Al_2O_3 . The elementary molecular structure is an aluminum octahedral structure [3]. Due to its environmental benignity, Fuller's earth is applied in the fields of drug delivery and wastewater treatment. The recently published volume of literature associated with Fuller's earth and its applications indicates an interest in using Fuller's earth in various applications, especially in wastewater treatment. Such wastewater management applications include adsorption techniques or augmentation with semiconductors to act as a photocatalyst. For instance, Safwat et al. [5] used Fuller's earth augmented with kaolin for the elimination of phenolic compounds from an aqueous stream via adsorption methodology. Moreover, Shah and his co-workers [9] used a modified form of Fuller's earth in combination with a surfactant to improve its adsorption capacity for eliminating acid red 17 dye from wastewater. However, to the best of the authors' knowledge, it has not been applied in its solo form as a photocatalyst for dye removal, especially as a source of the Fenton reaction. Catalysts from raw clay, such as Fuller's earth, could represent environmentally friendly and environmentally benign catalysts that possess many advantages. Such materials are cost-efficient and naturally abundant, in addition to being non-toxic to the environment, and they also possess excellent properties, such as a high surface area.

Fuller's earth clay is critical for creating $\cdot\text{OH}$ radical species, and this is achieved by using the elements in Fuller's earth, such as aluminum and iron ions [14]. Such ions react with hydrogen peroxide, and the reaction is initiated by ultraviolet light and then produces hydroxyl radicals. Iron and aluminum ions are formed and react with hydrogen peroxide to form further hydroxyl radicals and elemental ions (Equations (1) and (2)). $\cdot\text{OH}$ radicals are categorized as non-selective species that attack pollutant molecules and strongly oxidize them. Aluminum might initiate the Fenton reaction via the acyclic reaction [15].

A general trend of the aluminum-based Fenton reaction mechanism is the formation of the Al^{3+} superoxide complex (Equation (3)) [16]. In this reaction, the aluminum is able to stabilize a superoxide radical (O_2^- anion), and thus, the formed Al^{3+} superoxide complex (Equation (4)) is capable of reducing Fe^{3+} to Fe^{2+} . Hence, Fe^{2+} could enhance the production of $\cdot\text{OH}$ radicals through the Fenton reaction (Equation (5)) [17,18].



To the best of the authors' knowledge, according to the cited literature, "Fuller's earth" has not yet been applied as an oxidation source for pollutant remediation. Traditionally, clay sources are applied as adsorbent materials. Therefore, this investigative study introduces the novel application of Fuller's earth as the elemental source of Fenton oxidation. The goal of the current work is based on altering the traditional Fenton source with the environmentally benign, naturally available, and abundant clay "Fuller's earth", which comprises various metals. Such metals lead to Fenton reaction oxidation. The system is applied to mineralize Levafix Dark Blue aqueous effluent as a simulation of textile-effluent-polluted wastewater. The influence of various operating variables, i.e., Fuller's earth and the hydrogen peroxide reagent concentration, the pH of the medium, dye loading, and the temperature of the wastewater are assessed in order to meet the real application requirements.

2. Materials and Methods

2.1. Wastewater

Levafix Dark Blue dye, which is a kind of reactive azo dye, is commonly applied in the textile dyeing industry due to its high fastness profile, and it meets most requirements set by textile manufacturers. In this regard, commercial Levafix Dark Blue dye was used in the current study as a model synthetic pollutant. Thus, Levafix Dark Blue dye was used to prepare synthetic wastewater effluent. Levafix Dark Blue was supplied by DyStar Management Co., Ltd., Shanghai, China. The dye was used as received without further purification or treatment. The dye is dark blue and regarded as a bi-functional, combined anchor. The dye powder was used with no purification or further treatment. Initially, to attain the synthetic dye effluent, a stock solution of 1000 ppm of Levafix Dark Blue dye was prepared, which was then diluted, as required, for successive dilutions to obtain different concentrations according to the experimental conditions.

2.2. Preparation of Fuller's Earth-Based Fenton Catalyst

Naturally occurring Fuller's earth clay was collected from a deposit located in the southeastern desert in Egypt. After collection, the Fuller's earth clay was subjected to electric oven drying (105 °C) to remove any moisture content. Generally, the characteristics of clay, including its chemical and physical features, might be modified and enhanced through various treatments in order to improve its natural capacity to achieve better treatment results [14]. Such modifications could improve the physicochemical and mineralogical characteristics of the substance. Acid and thermal treatments of Fuller's earth are techniques widely applied to attain clay modification. Such techniques modify the mineralogical composition and chemical structure of Fuller's earth substance, as well as

leading to surface activation according to the authors' preliminary work. Thus, next, the Fuller's earth was ball-milled to attain a fine powder. Afterward, the material was sieved (200 mesh) and cooked with hydrochloric acid. Then, 15 gm of the material was cooked with 200 mL HCl acid (10 M) through heating (70 °C) and stirring for 1.5 h. Subsequently, the resultant aqueous media were successively washed with distilled water to reach a neutral pH. Subsequently, the solution was filtered, and the resultant solid powder was subjected to calcination (600 °C) for thermal activation purposes.

2.3. Photocatalytic Test

A stock solution of 1000 ppm was prepared from Levafix Dark Blue, and a further dilution was carried out when needed to obtain 50, 100, 150, and 200 ppm. Initially, 100 mL of the 100 ppm of Levafix Dark Blue dye-containing aqueous solution was poured into a glass container to subject it to the photocatalytic test. Then, a certain amount of Fuller's earth augmented with hydrogen peroxide (30% *w/v*) supplied by Sigma-Aldrich (Burlington, MA, USA) was poured into a container as the source of the Fenton photocatalyst and placed in a photochemical reactor. The mixture was magnetically stirred and kept under UV illumination after the pH was adjusted, if desired (using AD1030, Adwa instrument, Szeged, Hungary), over the range of 3.0 to 8.0. The pH of the dye aqueous solution was adjusted to the desired values by using diluted H₂SO₄ (1:9) and/or 1M NaOH solutions (Sigma-Aldrich). All chemicals were used as received from the supplier without further treatment or purification.

In order to validate the effect of the Levafix Dark Blue dye concentration on the extent of photocatalytic oxidation, the polluted water with the reagents was subjected to the photocatalytic system. A UV lamp (15 W, 230 V/50 Hz, with a 253.7 nm wavelength) was used to emit UV light during the reaction. The lamp was covered with a silica tube jacket for lamp protection, still allowing the UV to penetrate the dye-containing solution. The sleeved UV lamp was located inside a glass vessel containing the wastewater solution to well induce and accelerate the photocatalytic reaction. The photo-reactor had a 250 mL volume, and the reactor was fully exposed to UV light.

In regular time intervals (every 10 min), the samples were subjected to analysis after filtration (0.45 µm) to remove the remaining excess catalyst using a UV–visible spectrophotometer (Unico UV-2100, Franksville, WI, USA). The results of the analysis were recorded, and the data are presented as the dye percentage removal. The experimental setup is summarized in Figure 1.

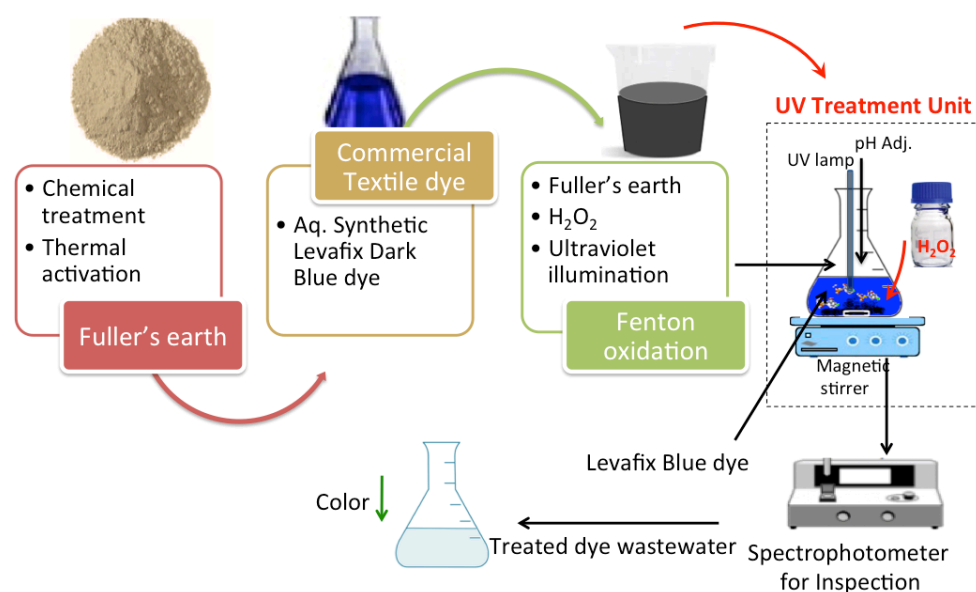


Figure 1. Schematic representation of the catalyst preparation and treatment steps.

2.4. Characterization Study

The morphologies of the attained Fuller's earth sample were explored and imaged using a field-emission scanning electron microscope (FE-SEM) (FE-SEM, Quanta FEG 250, Technical Cell, Kolkata, India). The typically used magnifications were $\times 8000$ and $\times 60,000$. Furthermore, this instrument was supplemented by energy-dispersive X-ray spectroscopy (EDX) in order to assess the content of principal oxides in the Fuller's earth. The oxides were examined via the energy-dispersive spectrum. Moreover, a Fourier transform infrared FTIR spectrum was obtained using the Jasco FT/IR-4100 model type (Jasco Inc., Mary's Court Easton, MD, USA).

2.5. Statistical Analysis

To attain a further higher reasonable dye removal efficiency with a good understanding of the roles of the significant independent parameters in the Levafix dye oxidation, a response investigated via dye percentage as dependent variable removal, a three-level factorial design, that is, the so-called Box–Behnken design, with triplicates of the central points, was applied. The selected independent variables were chosen according to the most affecting factors as follows: (i) H_2O_2 dose; (ii) Fuller's earth doses; and (iii) pH value. The levels and range for each parameter were selected according to a preliminary study that determined the manually optimized values. The selected levels and ranges are displayed in Table 1. Subsequently, SAS, statistical analysis software (SAS, Institute USA, Cary, NC, USA), was used to propose the full factorial experimental design matrix. Then, Matlab (7.11.0.584) software, as well as an analysis of variance (ANOVA), was chosen in order to analyze and specify the significance of the statistical technique. Moreover, Mathematica (V 5.2) software was selected in order to determine the optimal values. Finally, extra triplicates of the experiments were conducted to validate the proposed investigated model equation.

Table 1. Boundaries of the uncoded and coded experimental domains of the Box–Behnken factorial design with respect to their level spacing.

Experimental Variables	Symbols		Range and Levels		
	Uncoded	Coded	−1	0	1
H_2O_2 (mg/L)	ϵ_1	ζ_1	700	800	900
Fuller's earth (mg/L)	ϵ_2	ζ_2	0.75	1.0	1.25
pH	ϵ_3	ζ_3	2.5	3.0	3.5

3. Results and Discussion

3.1. Characterization of the Prepared Fuller's Earth Material

Scanning electron microscopy (SEM) was used to explain the treated and calcinated morphologies of the Fuller's earth material; an image is displayed in Figure 2. The surface was observed to have an irregular shape, and the clay possessed lots of asymmetric, open pores. The voids aid adsorption, as well as catalytic oxidation activity, a source of various metals. Moreover, elemental analysis techniques of the Fuller's earth material using an energy-dispersive X-ray analyzer (EDX) revealed its chemical composition, which constituted different oxides. The predominant oxide in the Fuller's earth was SiO_2 , as well as Al_2O_3 and Fe_2O_3 . The presence of Al_2O_3 and Fe_2O_3 leads to the occurrence of the Fenton reaction. Furthermore, trace amounts of CaO, MgO, K_2O , SO_3 , and Na_2O were present in the clay. A previous study [15] confirmed that the presence of Al_2O_3 leads to the Fenton reaction [18]. Moreover, various studies [15–18] verified that such oxides improve the adsorption tendency of Fuller's earth clay.

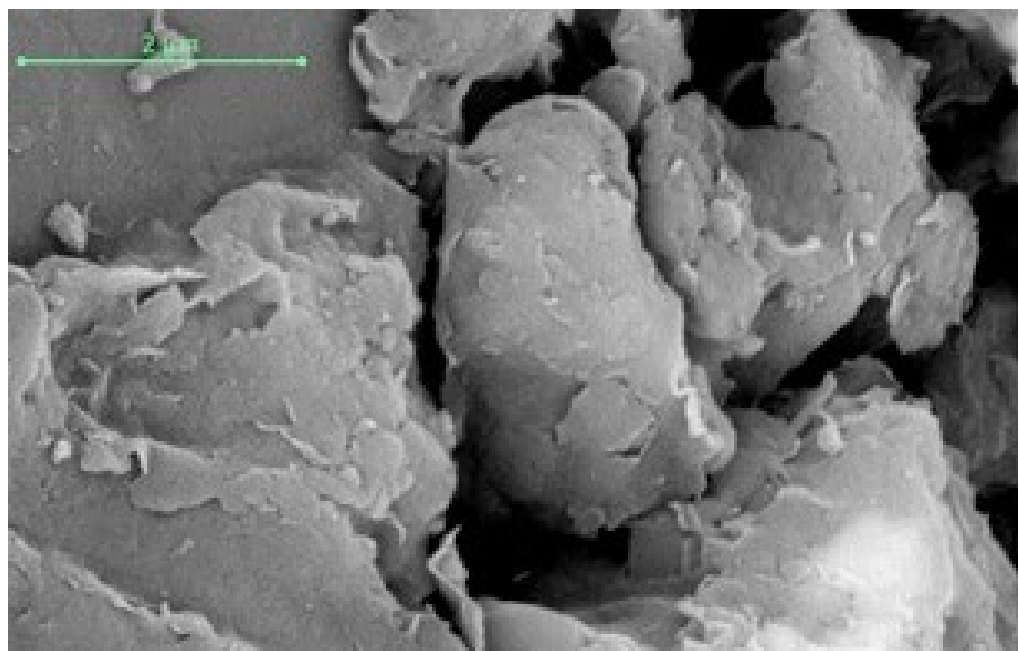


Figure 2. FE-SEM micrograph image of the prepared catalyst “Fuller’s earth clay”.

An oxide material analysis of the Fuller’s earth clay data obtained via an EDX analysis is displayed in Table 2. The main oxide of the chemically treated and then calcined modified Fuller’s earth powder was SiO_2 , along with Al_2O_3 and Fe_2O_3 , with the presence of small amounts of the oxides Ca, Mg, K, and Na. The use of Fuller’s earth, which is considered a clay, is due to its composition.

Table 2. Chemical oxide composition of modified Fuller’s earth determined via EDX.

Element	SiO_2	Al_2O_3	Fe_2O_3	CaO	MgO	K_2O	Na_2O	LOI
weight %	79.16	12.81	5.26	0.53	0.96	0.08	0.24	0.96

LOI: Loss of Ignition.

Although previous data [19] have indicated the importance of the oxides SiO_2 , Al_2O_3 , and Fe_2O_3 in enhancing the adsorption capacity of pollutants, Al_2O_3 and Fe_2O_3 are sources of the Fenton reaction [15–18]. Such oxides might be initiated through hydrogen peroxide to generate hydroxyl radicals, which are categorized as highly reactive intermediates and possess the ability to oxidize pollutant species [13].

A Fourier transform infrared (FTIR) transmittance spectrum analysis was applied as a suggestive technique. FTIR was applied to identify the different forms of minerals present in the Fuller’s earth that were introduced as a source for the Fenton oxidation test. Moreover, FTIR provided information on the chemical nature of the Fuller’s earth substance, as well as some details about the interactions. As illustrated in Figure 3, the FTIR performances of the Fuller’s earth clay exhibited coupled vibrations that are mainly due to the existence of numerous elements. Additionally, the main absorption-intensive bands of Fuller’s earth clay appeared. Silanol, which is characterized by Si–O stretching vibrations, is located at the 1034 cm^{-1} wavenumber. The occurrence of silanol represents the existence of quartz. Moreover, the bands at 528.4 cm^{-1} and 779 cm^{-1} are associated with the presence of illite, which is reflected by the Si–O–Al group. Moreover, the interlayer hydrogen bonding illustrates the possibility of hydroxyl linkage. Al–Mg–OH and Si–O–Fe bonding are reflected by the bands at 779 and 820 cm^{-1} , respectively. This confirmed the existence of Fe and Al bonding, which is necessary for the Fenton oxidation test.

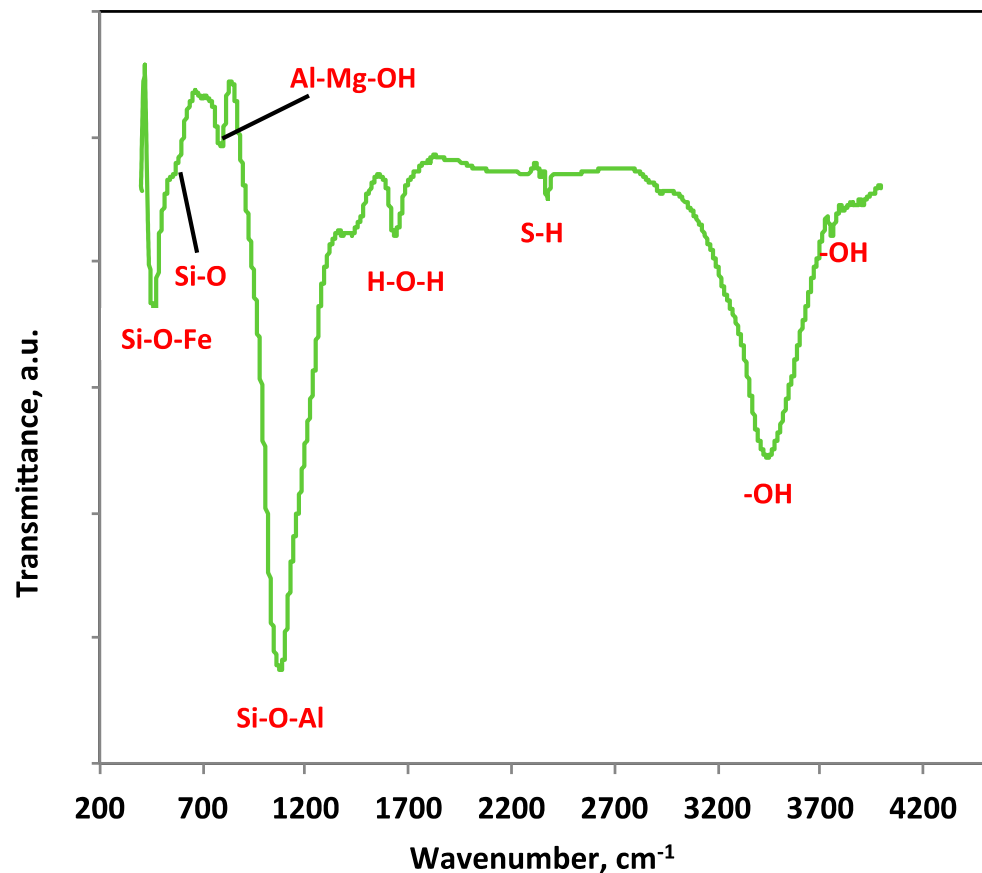


Figure 3. FTIR spectrum of the Fuller's earth clay.

3.2. Reactive Azo Dye Oxidation

3.2.1. Effects of Reaction Time and Reactive Azo Dye Loading

Each of the experimental parameters affecting the kinetics of the reaction was investigated, starting with the experimental reaction time. In this experiment, the influence of the oxidation system was examined in terms of the photo-Fenton oxidation reaction based on Fuller's earth natural clay. In order to examine the optimal reaction time and its impact on the oxidation process, experiments were undertaken with illumination times ranging from 2 to 60 min. All other parameters, including the initial concentrations of Fuller's earth and H_2O_2 at 1.0 g/L and 800 mg/L, respectively, were kept constant, and the solution pH was maintained at 3.0. Figure 4 demonstrates the influence of the reaction time on the profiles of various reactive azo dye loadings. An investigation of the results in Figure 4 indicated that the dye oxidation rate reached 73% within only the initial two minutes of the illumination time. However, afterward, it steadily declined, achieving an accumulative oxidation efficacy reaching 97% within 15 min when the initial azo dye concentration was 50 mg/L. According to the previously cited literature [16,20], azo dye molecules compromise aromatic rings. The hydroxyl radicals generated from the reaction of Fuller's earth with hydrogen peroxide attack such rings and open them. Then, this generates reaction intermediates and eventually oxidizes them to harmless end products (CO_2 and H_2O). Initial rapid oxidation was dominant for all the dye concentrations. As the reaction proceeded, the generated hydroxyl radicals in the reaction medium gradually declined, corresponding to a reduction in the H_2O_2 concentration. Moreover, radicals other than hydroxyl radicals were produced, and they inhibited the oxidation reaction rate rather than improving the dye removal rate. The previous conclusion by [13] confirmed this investigation by treating various dyes contaminating wastewater effluent.

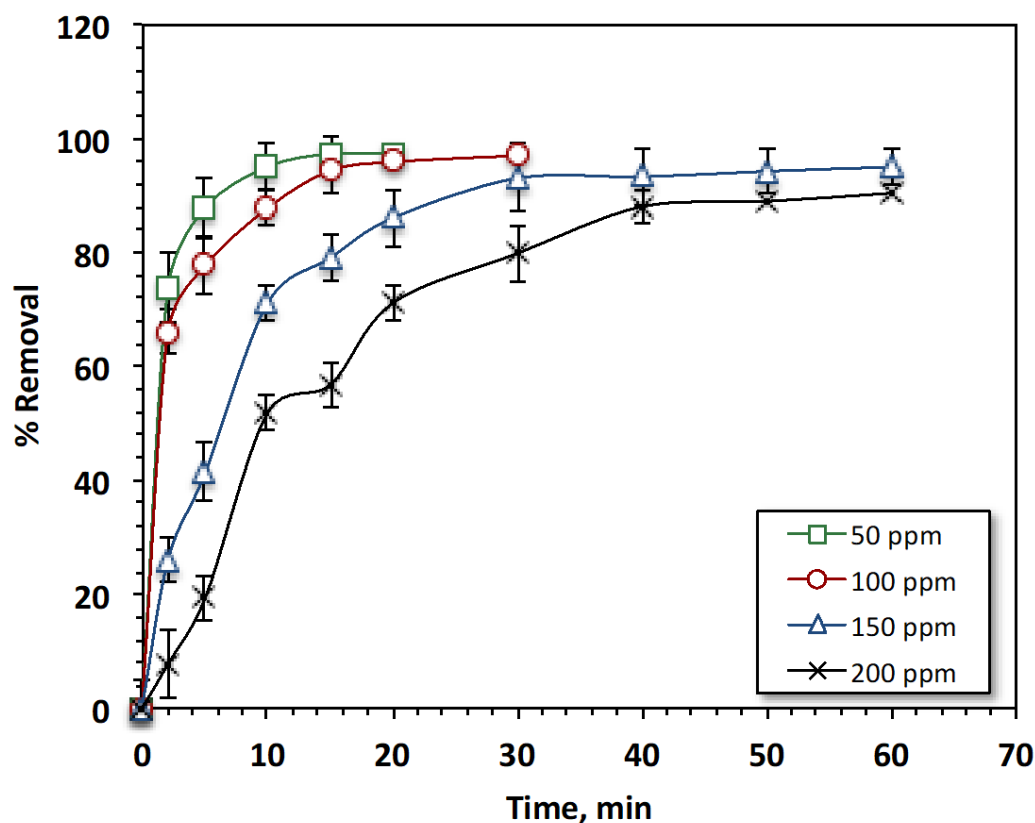


Figure 4. Effects of azo dye Levafix Dark Blue loadings on the oxidation reaction (experimental conditions: Fuller's earth 1.0 g/L; H₂O₂ 800 mg/L; and pH 3.0).

While a similar rapid reaction rate in the initial reaction time period was observed for all the treated dye concentrations, an assessment of Figure 4 found that the oxidation rate declined with the increase in the dye loading. The removal efficiencies were 97, 95, 91, and 79% for the 50, 100, 150, and 200 mg/L azo Levafix Dark dye concentrations in the aqueous effluent, respectively. Moreover, the reaction time also increased from 20 to 100 min with the increase in the dye loading. At higher dye concentrations, the concentration of the exerted $\cdot\text{OH}$ radicals was insufficient for completing dye oxidation. This conclusion of increasing the oxidation activity with a reduction in the initial pollutant concentration was also previously investigated and recorded by Raut-Jadhav et al. [21], who used the Fenton reagent for the oxidation of methomyl-pesticide-containing wastewater.

3.2.2. Effects of Various Treatment Systems

The effects of various treatments based on oxidation systems, namely, Dark/Fuller earth, Dark/H₂O₂, Dark/H₂O₂-Fuller earth, UV/H₂O₂, UV/Fuller earth, and UV/H₂O₂-Fuller earth, were explored to test the effect of the Fenton reaction tendency using Fuller's earth as a catalyst. The efficacy of these techniques was assessed in terms of Levafix Dark Blue dye color removal, and the results are exhibited in Figure 5. The data compare the Levafix Dark Blue oxidation using the different systems at room temperature. It is clear from the data in Figure 5 that the solo H₂O₂ oxidation system results in the dye having oxidation efficiencies of only 7% and 38% in the dark and under ultraviolet illumination, respectively, within 20 min of the reaction time. Moreover, in the dark test and under UV illumination, the solo Fuller's earth catalyst reached removal efficiencies of 26 and 39%, respectively. However, under the solo UV illumination system, the dye oxidation reached a removal rate of only 11%. In contrast, the augmented Fuller's earth with hydrogen peroxide oxidative treatment could mineralize the dye to attain rates of 72 and 98% in the dark and under UV illumination, respectively. It is worth mentioning that the photo-Fenton system based on Fuller's earth augmented with hydrogen peroxide achieved the highest oxidation among

the investigated oxidation systems. Notably, the high removal rates of the Fenton system or the photo-Fenton system compared to those of the solo hydrogen peroxide systems or the Fuller's earth systems verify the role of the Fenton reaction in eliminating dye molecules. The presence of dual reagents might explain this in the Fenton system, as they support the generation of more hydroxyl radicals. Moreover, the presence of ultraviolet light results in further hydroxyl radical production, which is the main responsibility of the oxidation system. This reaction trend was previously reported by Thabet et al. [13], who treated contaminated dye effluent using a modified Fenton system.

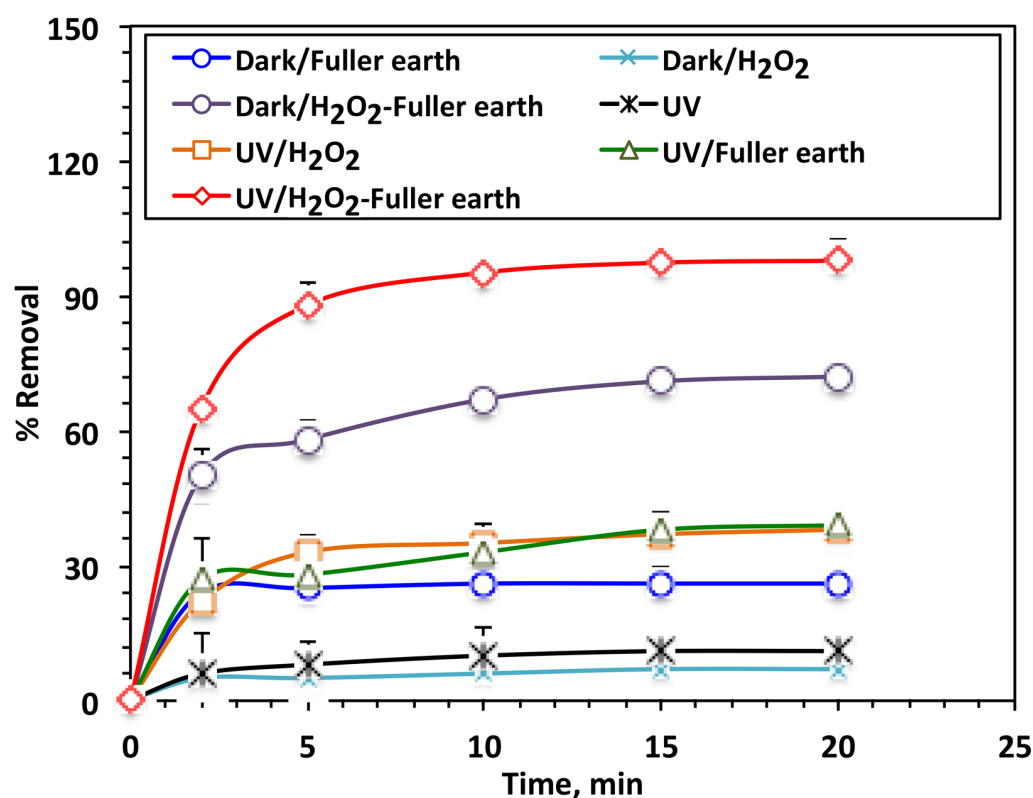


Figure 5. Effects of different treatment systems on azo dye Levafix Dark Blue (experimental conditions: azo dye Levafix Dark Blue 50 ppm; Fuller's earth 1.0 g/L; H₂O₂ 800 mg/L; and pH 3.0).

However, with an increase in time, the Levafix Blue dye removal exhibited a slower rate since $\cdot\text{OH}$ radical production declined. Contrary, a rapid initial stage of oxidation was achieved. This is due to the consumption of the reagent in the initial stage to produce hydroxyl radicals [22]. The oxidation occurred by utilizing the activation of H₂O₂ with the metal salts present in Fuller's earth in the case of the Fenton system. However, by exceeding the reaction time, a reduction in the dye rate was attained that corresponded to the decline in the presence of H₂O₂. This is related to the hydroxyl radical formation. Moreover, this phenomenon is also exhibited in hydrogen peroxide-based systems since the amount of hydrogen peroxide reduces due to it being consumed as time proceeds. Various research data [23] have exhibited that the quick initial reaction time is due to the immediate generation of $\cdot\text{OH}$ radical species. Furthermore, the lower oxidation tendency of the dark reaction test is associated with the absence of UV illumination. Thus, it initiated oxidation through the generation of more $\cdot\text{OH}$ radical species. Remarkably, the Fuller's earth catalyst is easily available since it is naturally abundant as a sustainable substance.

3.2.3. Effects of Photo-Fenton Parameters

Effect of Fuller's Earth Dose

To examine the effect of the Fuller's earth catalyst, as a source of the Fenton reaction, on the Fenton oxidation of azo dye, experiments were undertaken to investigate the influence

of clay dose on the reaction kinetics. Figure 6 displays its influence on the oxidation reaction by varying the Fuller's earth concentration over the range of 0.5 to 1.5 mg/L.

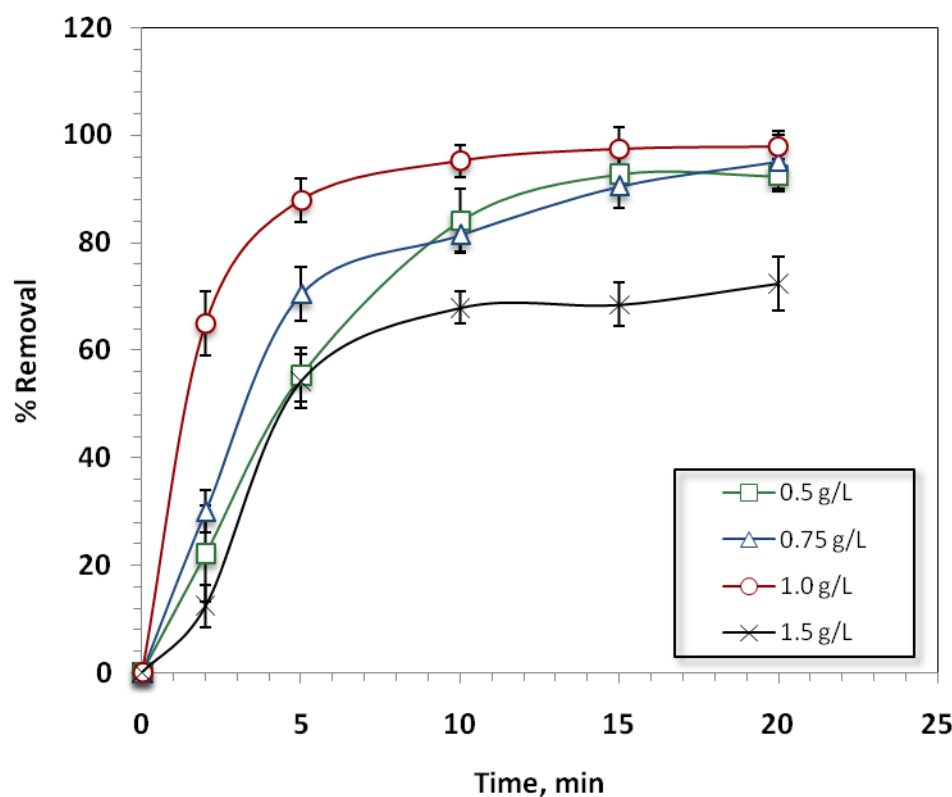


Figure 6. Effect of Fuller's earth concentration on photo-Fenton oxidation system (experimental conditions: azo dye Levafix Dark Blue 50 ppm; H_2O_2 800 mg/L; and pH 3.0).

The oxidation removal efficacy was enhanced (from 92% to 97%) by increasing the Fuller's earth dose from 0.5 to 1.0 mg/L. However, further increasing Fuller's earth to 1.5 mg/L resulted in a significant decline in dye oxidation, reaching only 72%. This could be associated with the Al and Fe ions that form in the aqueous solution since they are present in Fuller's earth and then react with H_2O_2 to form further OH radicals and metal ions. These non-selective 'OH radicals attack the dye molecules and strongly oxidize them. However, a further increase in the Fuller's earth catalyst resulted in a decline in the oxidation efficiency as a result of the shadowing effect arising from the turbid solution. This phenomenon of shadowing the UV illumination is due to the Fuller's earth comprising inorganic materials that obey UV transmittance when it is in excess. Additionally, an excessive concentration of metal ions results in their acting as 'OH radical scavengers rather than generators according to the abovementioned equations (Equation (5)). This investigation is in accordance with the studies in [24–28], in which organic materials and dyes from wastewater are treated via the Fenton reaction.

Effect of Hydrogen Peroxide Reagent Concentration

Figure 7 displays the reactive dye Levafix Dark Blue oxidation in the presence of the Fuller's earth-based photo-Fenton system. The oxidation rates elevated when the H_2O_2 reagent dose was increased from 200 to 800 mg/L, until reaching practically 97% Levafix Dark oxidation. This occurred with a 20 min illumination time using the optimal value of 800 mg/L of H_2O_2 , 1 g/L of Fuller's earth, and a solution pH of 3.0. This increase in the removal efficiency with the increase in the reagent is associated with the production of more peroxide species and hydroxyl radicals in the aqueous medium. These radicals are the horsepower of the oxidation reaction, as well as its main responsibility. Moreover, elevating the H_2O_2 concentration to 1000 mg/L, more than the optimal limit (800 mg/L),

affects the reaction rate and results in a decline in oxidation, reaching only 74%. This is probably related to the excess reagent concentration of ion pairs on the surface that could reduce the availability of the Fuller's earth elemental sites to react with the excess H_2O_2 (Equations (6) and (7)). In such a situation, additional H_2O_2 may have a detrimental effect due to the scavenging of hydroxyl radicals that occurs at higher H_2O [24]. Moreover, there are radicals other than OH radicals in the presence of excess hydrogen peroxide; such radicals inhibit the oxidation reaction (Equations (8) and (9)).

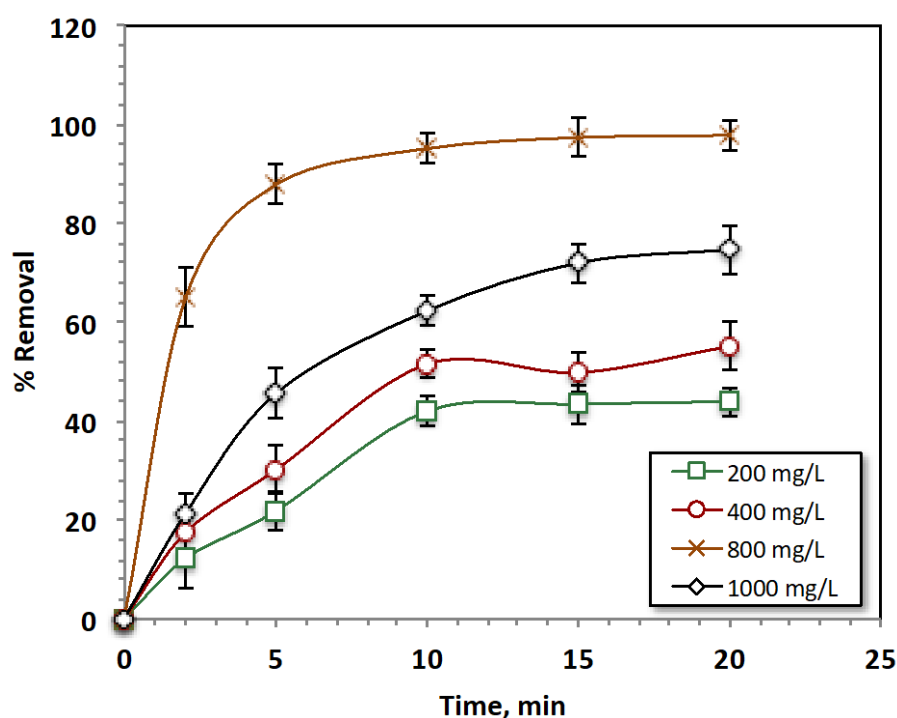
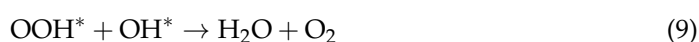
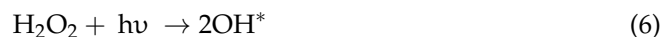


Figure 7. Effect of hydrogen peroxide concentration on photo-Fenton oxidation system (experimental conditions: azo dye Levafix Dark Blue 50 ppm; Fuller's earth. 1.0 g/L; and pH 3.0).

Effect of pH Value on the Treatment Efficiency

The pH of the aqueous environment is categorized as a vital influencing variable in Fenton oxidation. This demonstrates its importance since the pH influences H_2O_2 decomposition and the hydrolytic speciation of metal ions. In this regard, to evaluate its influence on the Levafix Dye oxidation through the modified photo-Fenton system, the initial pH values were altered from an acidic value to an alkaline value to evaluate their effects on the system. The pH values varied over the range of 3.0 to 8.0 according to the results displayed in Figure 8; an alkaline pH value is not favorable for the oxidation reaction using the photo-Fenton system. However, further oxidation was achieved when the acidic pH was used. Notably, it was obvious that the acidic pH (3.0) value of wastewater attained the highest removal efficiency. The removal efficiency reached 97% within 20 min of the illumination time, at which point the Levafix dye oxidized into other intermediates. However, increasing the aqueous solution pH to an alkaline pH value results

in the presence of excess unfavorable ions. Such ions react with superoxide species rather than the metals in the catalyst. This hinders the overall reaction. These metals are mostly accountable for provoking H₂O₂ to produce (OH) radicals [27]. The result is the formation of the hydroperoxide (HO₂) inactive radical, which reduces the oxidation efficacy [28]. Hence, the Levafix oxidation yield further declined at an alkaline pH. The findings of this investigation of the low efficiency at a high pH are in accordance with the previous findings of Nichela et al. [15], who treated a nitrobenzene-contaminated aqueous stream using a Fenton-based reaction.

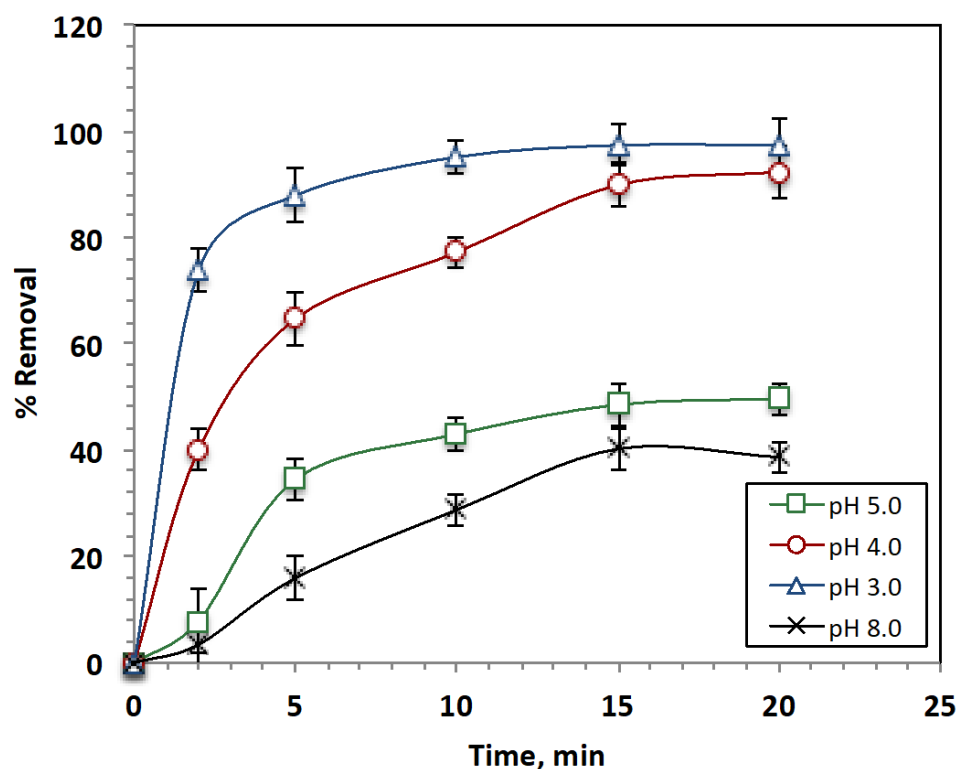


Figure 8. Effect of pH value on photo-Fenton oxidation system (experimental conditions: azo dye Levafix Dark Blue 50 ppm; Fuller’s earth 1.0 g/L; and H₂O₂ 800 mg/L).

Box–Behnken Regression Design Fitting

RSM, response surface regression methodology, was applied to explore the operational parameters’ optimal values for the modified photo-Fenton system based on the Fuller’s earth clay system. These parameters include the Fuller’s earth clay and hydrogen peroxide concentrations, as well as the pH value, in order to maximize the Levafix dye efficacy removal. The used outlined matrix is tabulated in Table 1, as well as the experimental dye response after the oxidation reaction, with the predictive model values presented using Equation (10). This equation exploring the second-order polynomial regression model exhibits the response surface in terms of the coded variables for the Levafix dye removal response.

$$Y(\%) = 90.47 + 2.28 \varepsilon_1 - 4.68 \varepsilon_2 - 5.08 \varepsilon_3 - 4.75 \varepsilon_1^2 + 0.23 \varepsilon_1 \varepsilon_2 - 12.57 \varepsilon_1 \varepsilon_3 - 4.98 \varepsilon_2^2 + 6.3 \varepsilon_2 \varepsilon_3 - 18.41 \varepsilon_3^2 \tag{10}$$

An ANOVA test based on Fisher’s statistical analysis was performed for the assessment of the statistical consequence and the adequacy of a quadratic model. With a minimum deviation, a small probability value (<0.005), and a high R² (the regression coefficient value), the model was shown to be the best fit. The R² value of the Levafix Dark dye oxidation response was 94.3%.

A graphical representation of the abovementioned equation (Equation (10)) demonstrates the influences of the experimental parameters on the response. The 3-D (three-dimensional) surface and the 2-D (two-dimensional) contour plots of the operational parameters were designed using Matlab software, and the results are displayed in Figure 9a–c. The data displayed in the figure revealed the response of each experimental influencing variable and the major interactions between those variables. An inspection of the 3-D surface graph and the 2-D contour plot in Figure 9b illustrated that the removal rate of the Levafix dye was enhanced with the increase in the concentrations of both H_2O_2 and Fuller’s earth. However, the curvature displayed in Figure 9a indicates that there is a significant interaction effect between the Fuller’s earth and hydrogen peroxide doses. This interaction encourages the generation of hydroxyl radical species that have a positive effect on the dye removal rate. Nevertheless, a further increase in the concentrations of both reagents resulted in a reduction in the dye oxidation rate. Thus, an optimal ratio of Fuller’s earth/ H_2O_2 is essential to increase the yield of ($\cdot\text{OH}$) radicals [27].

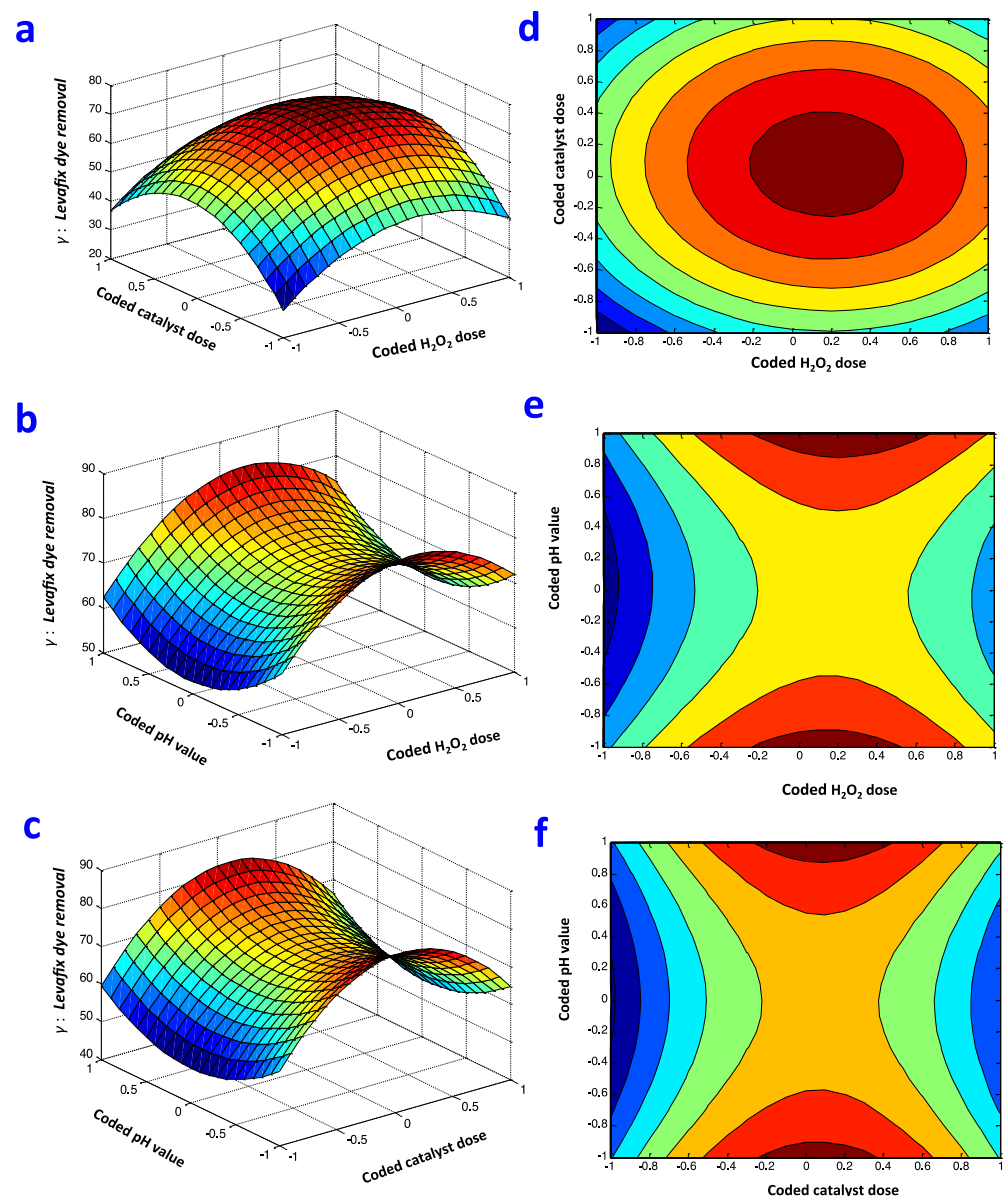


Figure 9. The 3-D (a–c) and 2-D (d–f) surface and contour plots of the coded independent variables and their responses in Levafix Dye removal: (a) H_2O_2 and Fuller’s earth catalyst concentrations; (b) H_2O_2 concentration and pH; (c) Fuller’s earth catalyst concentrations and pH.

Figure 9b explains the influence of the Fuller's earth catalyst dose and the significant parameter of pH in the augmented 3-D and 2-D response surface and contour plots. The graph confirms that the oxidation efficiency enhanced with an increasing catalyst dose. However, an alkaline environment is not favorable for Levafix oxidation. The optimum pH is near the acidic pH 3.0. The existence of scavenger species is apparent in the reaction medium rather than the reactive hydroxyl radicals in the reaction media. So, the result is a reduction in the overall reaction of oxidation, clarifying this finding.

The combined 3-D and 2-D response surface and contour plots displayed in Figure 9c demonstrate the influences of the independent hydrogen peroxide and pH values, respectively, on the Levafix dye as azo dye removal rates. An investigation was carried out on the figure results of Levafix Dye oxidation. In this set of experiments, the pH varied over the range of 2.5–3.5. The surface and contour plots of the RSM show that the highest percentage of dye removal was obtained at the intersection near the origin of the two variables.

For an extra examination of the proposed model, the statistically optimized predicted parameters investigated using Mathematica software were examined. The optimal conditions revealed from the predicted model were 818 mg/L, 1.02 mg/L, and 3.0 for H₂O₂, Fuller's earth catalyst, and pH, respectively. Then, an extra three replicates of experiments were carried out to confirm the predicted values' adequacy. After a 2 min reaction time, the measured percentage of dye removal (71%) was close to the predicted value (72%), which was obtained by applying the suggestive factorial design. Moreover, the overall oxidation reaction reached a 99% dye removal rate within 15 min of the reaction time. This investigation verifies that the response surface methodology is a satisfactory approach for optimizing the operational parameters' influence using the Fuller's earth-based Fenton system.

3.2.4. Effect of Temperature

In catalytic illumination oxidative systems, temperature is considered a vital parameter that affects reaction rates. To explore the influence of temperature on the reaction kinetics, Levafix Dark Blue dye oxidation experiments over a temperature range from 25 °C to 60 °C were undertaken. The results in Figure 10 display superior oxidation leading to an increase in the Levafix Dye removal efficacy, achieving complete removal with a shorter reaction time when the temperature is elevated.

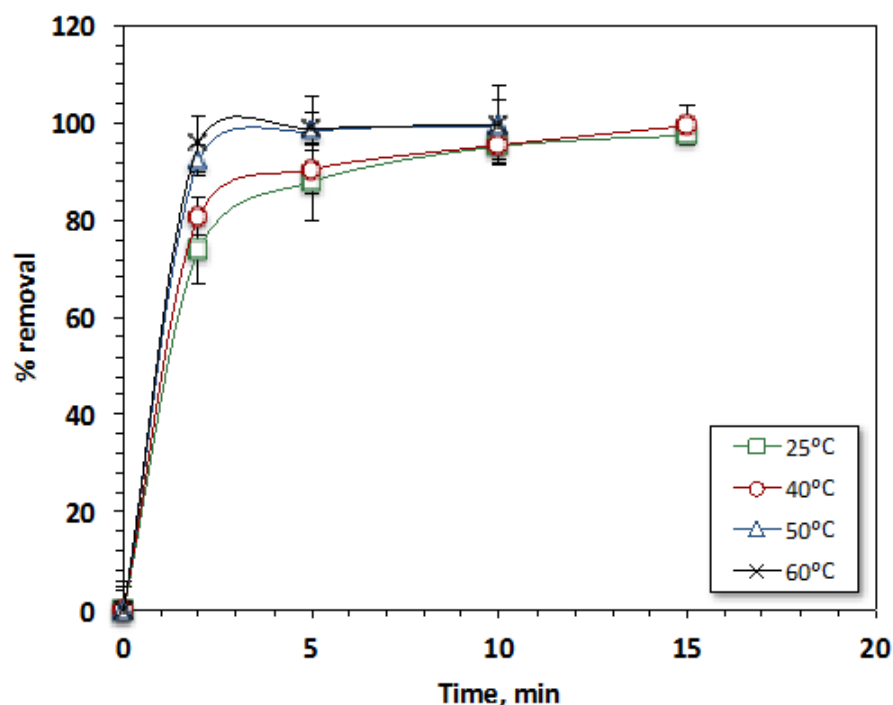


Figure 10. Temperature effect on Levafix removal via Fullers' earth-based Fenton process.

An examination of Figure 10 found that elevating the temperature from 25 °C to 60 °C for the aqueous Levafix solution attained a shorter reaction time of only 10 min and an enhancement from 97% to 100%. According to the previously cited literature [24], reaction rates are normally more efficient at higher temperatures. The various data cited in the literature [29,30] show that temperature elevation has a positive effect on Fenton systems for some wastewater-treated effluents.

3.2.5. Kinetics and Thermodynamics

In this section, the reaction kinetics and thermodynamics of Levafix dye oxidation via the photo-Fenton-modified system are investigated. In the current study, the photo-Fenton oxidation kinetics of Levafix dye using a modified reaction, the Fuller's earth-based photo-Fenton process, was evaluated for various contact times varying from 0 to 20 min under isothermal conditions at the following operating temperatures: 25, 40, 50, and 60 °C. Moreover, the zero-, first-, and second-order reaction kinetics were assessed for the modified Fenton oxidation reaction according to the following equations: Equation (11) for the zero-, Equation (12) for the first-, and Equation (13) for the second-order reaction kinetics [31]:

$$C_t = C_o - k_0t \quad (11)$$

$$C_t = C_o - e^{k_1t} \quad (12)$$

$$\left(\frac{1}{C_t}\right) = \left(\frac{1}{C_o}\right) - k_2t \quad (13)$$

where C is the concentration of the Levafix dye; C_t is the concentration of the Levafix dye at time t ; C_o is the Levafix dye's initial concentration; t is the reaction time; and k_0 , k_1 , and k_2 represent the kinetic rate constants for the zero-, first-, and second-order reaction kinetics, respectively.

The reaction kinetics most appropriate for Levafix removal were assessed by plotting Equations (11)–(13) for the experimental results data. The kinetic parameters, as well as the regression coefficients (R^2), for each reaction order were investigated, and the data are tabulated in Table 3. Examining the data in Table 3 revealed that the reaction is well-fitted to a second-order reaction. Further, the kinetics constant of the second-order reaction constant, k_2 , was notably affected by the reaction temperature, increasing with the temperature elevation. This investigation is associated with the generation of the 'OH species since it is a product of the reaction of Fuller's earth with hydrogen peroxide. Moreover, another kinetics value of importance is $t_{1/2}$ (the half-life of a reaction), which signifies the essential time needed for the reactant's initial concentration to decrease by half. An examination of Table 3 revealed that the calculated $t_{1/2}$ is a function of the reaction temperature; $t_{1/2}$ declines with increasing temperature. Various researchers in other studies have confirmed that the Fenton reaction follows second-order reaction kinetics.

To fully understand the modified Fenton reaction based on the use of Fullers' earth oxidation to oxidize Levafix dye molecules, thermodynamic parametric data were quantified. Arrhenius formula was used to investigate the activation energy, $k_2 = Ae^{\frac{-E_a}{RT}}$, with the activation energy (E_a) of the Levafix dye oxidation being based on the second-order kinetic constant, where R is the gas constant ($8.314 \text{ J mol}^{-1}\text{K}^{-1}$), T is the temperature in kelvin, and A is the pre-exponential factor that is considered to be constant with respect to temperature [32]. Taking the natural log of the Arrhenius formula yields the following:

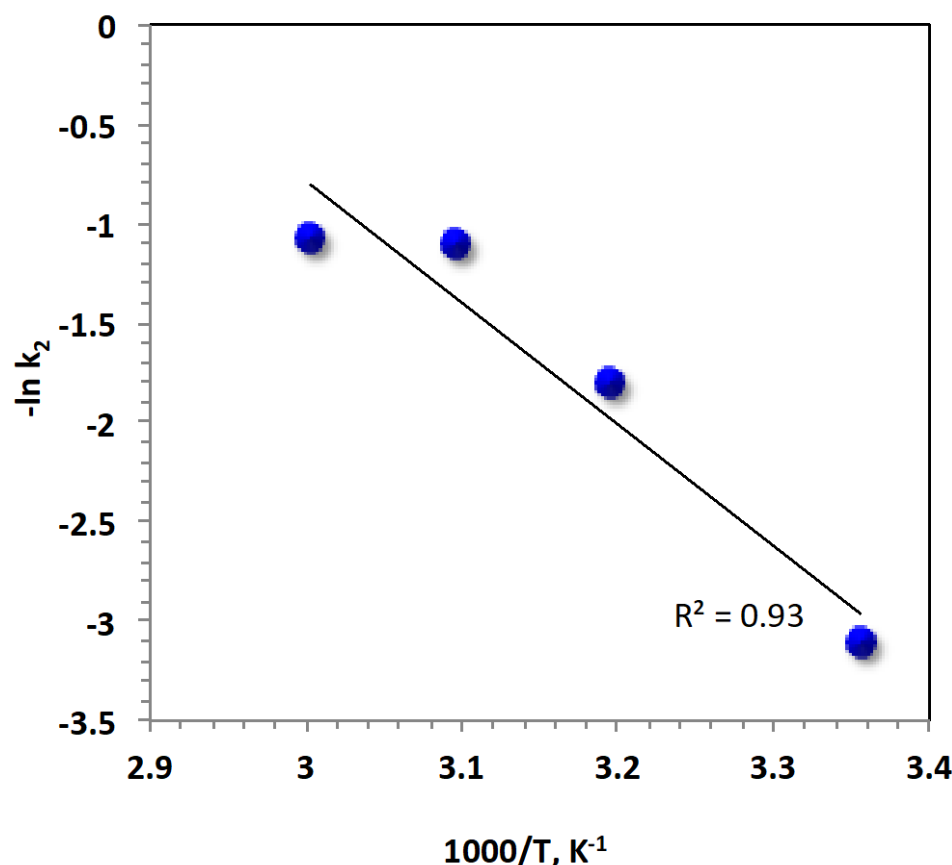
$$\ln k_2 = \ln A - \frac{E_a}{RT} \quad (14)$$

Table 3. Fitted rate constants for the oxidation reaction of dye-containing wastewater *.

Kinetic Model	Parameter	Temperature, °C			
		25	40	50	60
Zero-order	k_0 (mg.min ⁻¹)	2.673	2.62	2.459	2.403
	$t_{1/2}$ (min)	72.171	70.794	66.393	64.881
	R^2	0.54	0.49	0.39	0.37
First-order	k_1 (min ⁻¹)	0.223	0.293	0.33	0.317
	$t_{1/2}$ (min)	3.107	2.365	2.100	2.186
	R^2	0.90	0.94	0.81	0.72
Second-order	k_2 (L.mg ⁻¹ min ⁻¹)	0.044	0.164	0.328	0.341
	$t_{1/2}$ (min)	0.4208	0.1129	0.0564	0.0543
	R^2	0.97	0.90	0.98	0.97

* k_0 , k_1 , k_2 : kinetic rate constants of zero-, first-, and second-reaction kinetic models; C_0 and C_t : dye concentrations at initial time and time t ; t : time; R^2 : correlation coefficient; $t_{1/2}$ half-life time.

A plot of $\ln k_2$ versus $1/T$ could be used to investigate the value of E_a (Figure 11). Figure 11 displays the relationship of the Levafix Dark Blue dye oxidation through the modified Fuller's earth-based photo Fenton system reaction. The value of E_a of the process was recorded to be 50.8 KJ mol⁻¹.

**Figure 11.** Plot of $\ln k_2$ versus $1000/T$ for the modified Fuller's earth Fenton system.

Other various thermodynamic variables, such as the enthalpy ($\Delta H'$), entropy ($\Delta S'$), and free energy ($\Delta G'$) of activation, were assessed utilizing Eyring's equation with the utilization of E_a and k_2 values according to the following relation [24]:

$$k_2 = \frac{k_B T}{h} e^{\left(-\frac{\Delta G'}{RT}\right)} \quad (15)$$

where k_B is the Boltzmann constant, and h is Planck's constant. The thermodynamic parameters for Levafix dye oxidation were estimated accordingly, and they are displayed in Table 4.

Table 4. Thermodynamic properties of organics removal using modified Fuller's earth Fenton oxidation.

Parameters Thermodynamic Parameters	Temperature (°C)			
	25	40	50	60
$\Delta G'$ (kJ/mol)	80,720.78	81,487.94	82,314.45	84,839.69
$\Delta H'$ (kJ/mol)	−2426.76	−2551.47	−2634.61	−2717.75
$\Delta S'$ (J/mol)	−279.02	−268.49	−263.00	−262.93
E_a (kJ/mol)	50.8			

An investigation of the data in Table 4 found that the positive values of $\Delta H'$ across the studied temperature range indicate that the reaction is endothermic. Moreover, $\Delta G'$ exhibited positive values, which means that the process is non-spontaneous. This result might be because of the formation of a well-solvated structure between the dye molecules and the OH radical species. Moreover, the negative entropy values also support this.

3.2.6. Catalyst Stability and Reusability

To investigate the adequacy of the catalyst activity, its cyclic use was examined. To assist this investigation, the catalyst was collected after each use, washed with distilled water, and then subjected to oven drying for 1 h (105 °C). The catalyst loss was calculated, and it did not reach more than 1%. Then, the recovered catalyst was used for dye treatment at the optimal reagent doses of 818 mg/L, 1.02 mg/L, and 3.0 for H_2O_2 , the Fuller's earth catalyst, and pH. The catalyst was repeatedly used, and its efficiency for treatment was examined. The catalyst reactivity reduced, achieving only 73% dye removal in the sixth cycle compared to the 99% achieved with the use of the fresh catalyst, as shown in Figure 12. However, it is worth mentioning that the catalyst was still efficient in removing dye from the aqueous solution. This reduction in the catalyst efficiency could be associated with the dye molecules occupying the active sites of the catalyst surface. Thus, its efficiency in producing hydroxyl radicals is reduced, and they are the horsepower of the oxidation reaction. Such a reduction in the catalyst efficacy after multiple uses has previously been reported in the literature [6] investigating the magnetized biomass catalyst recyclability in treating polluted wastewater.

It is worth mentioning that various researchers [6,11,33] have suggested that using a solvent for dye desorption might result in the regeneration of the catalyst. Moreover, eliminating the dye molecules occupying the catalyst surface through temperature elevation might also regenerate the catalyst. Additionally, changing the pH of the medium to achieve dye desorption could facilitate catalyst regeneration [34]. Moreover, introducing supercritical CO_2 to substitute the organic solvents for the desorption ability is a promising technique since it overcomes the environmental concerns regarding hazardous solvents. These suggested methods might elaborate the stability and recyclability of Fuller's earth. Not only can these methods regenerate the Fuller's earth material, but they can also recover and enable the collection of the dye adsorbate rather than destroying it, which is suggested to be an ideal sustainable solution. Therefore, these techniques are recommended for improving catalyst regeneration.

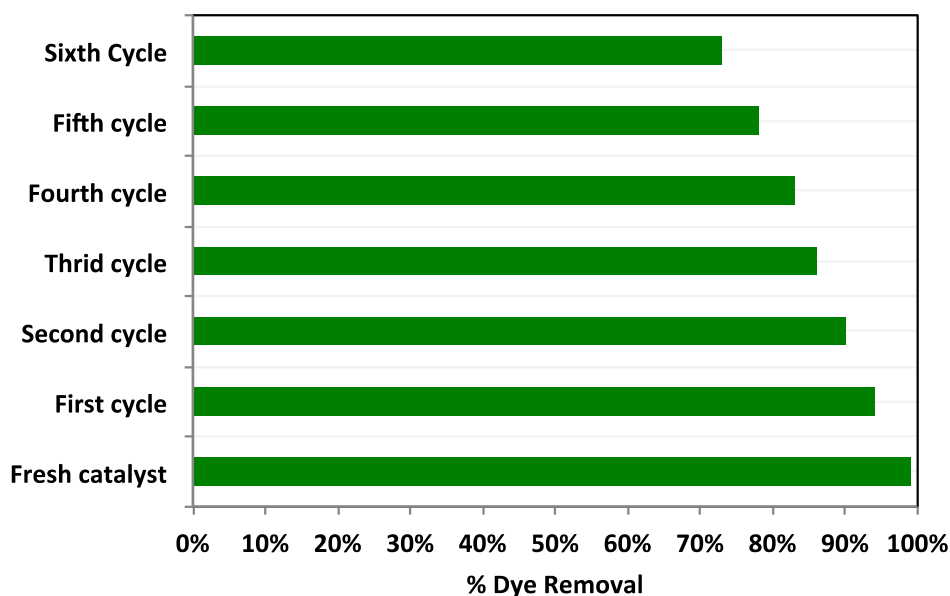


Figure 12. Catalyst reusability efficiency for cyclic use.

3.2.7. Data Comparison with Previous Fenton Studies

A comparison of various data presented in previous studies cited in the literature using the Fenton reaction to treat various types of dyes was carried out, and the results were compared with those of the current investigation. The comparison study is based on the modified Fenton system to examine the adequacy of the modified current study, and the comparison data are exhibited in Table 5. Regarding the oxidation removal efficiencies of the different processes, according to the data tabulated in Table 5, the Fenton reagent could achieve almost complete oxidation of various dye types. However, some systems are characterized by a low efficiency, such as the $\text{H}_2\text{O}_2/\text{Fe}$ -zeolite and $\text{H}_2\text{O}_2/\text{Co-Fe}_2\text{O}_4$ systems. Additionally, it is worth mentioning that, in the current study of the modified Fenton system based on the use of Fullers' earth as a naturally occurring catalyst, only a limited time is needed in the current investigation for the reaction (20 min) compared to the other systems. Moreover, the current modified Fenton system is an efficient, superior mode of treatment since it is based on a naturally abundant material that is considered a minimal or costless catalyst. Thus, this current suggestive study is much better and cheaper, especially when the Fullers' earth catalyst is used as the source of the photo-Fenton system. Additionally, the process is environmentally friendly compared to the other techniques listed in Table 5, as they are not based on the use of naturally occurring substances as catalysts.

Although the other oxidation reactions also exhibited high dye removal efficiencies that almost resulted in complete removal, it is significant to mention that the catalyst source in the other studies was a metal-based synthesized catalyst. In the current study, the catalyst was based on a naturally abundant material. The efficiency of the current method being higher than that of the other Fenton technologies in Table 5 might also be associated with the occurrence of multiple metals in the catalyst, which increases the oxidation rate. Further, the catalyst dose in the current investigation was quite reasonable in comparison to that in the other studies, and the hydrogen peroxide reagent was not quite as high, with some studies reaching 2720 mg/L. However, in the other studies, only a minimal amount of hydrogen peroxide was essential, reaching 0.68 mg/L. Moreover, a higher reaction time was essential, reaching 150 min with a treatment efficiency of 79%. Additionally, it is worth mentioning that such data are attained when applying a costless, naturally abundant catalyst in treatment in comparison to the other mentioned systems in Table 5. Typically, the use of natural materials is superior in treatment due to their advantages of having environmentally benign characteristics.

Table 5. Comparing efficiency of various Fenton-based systems in oxidizing dyes.

Fenton System	Target Dye Pollutant	Initiation Source	Operating Conditions	Oxidation Time	Efficiency	Ref.
H ₂ O ₂ /Fullers' earth	Levafix blue	Ultraviolet illumination	Catalyst 1.02 g/L; H ₂ O ₂ 818 mg/L; pH 3.0; Temperature 298 K	20 min	99%	Current work
H ₂ O ₂ /Clay-Fe ₃ O ₄	Levafix blue	Ultraviolet illumination	Catalyst 1 g/L; H ₂ O ₂ 400 mg/L; pH 3.0; Temperature 300 K	30 min	100%	[13]
H ₂ O ₂ /Fe-laponite	Acid Black 1	Ultraviolet illumination	Catalyst 1 g/L; H ₂ O ₂ 218 mg/L; pH 3.0; Temperature 298 K	120 min	100%	[34]
H ₂ O ₂ /Fe-zeolite	Acid Blue 74	Ultraviolet illumination	Catalyst 0.3 g/L; H ₂ O ₂ 228 mg/L; pH 5.0; Temperature 298 K	120 min	55%	[35]
H ₂ O ₂ /Fe _{2.46} Ni _{0.54} O ₄	Methylene blue	Dark Fenton	Catalyst 1.0 g/L; H ₂ O ₂ 340 mg/L; pH 7.0; Temperature 298 K	50 min	10%	[36]
H ₂ O ₂ /Co-Fe ₂ O ₄	Methylene blue	Natural solar radiation	Catalyst 0.2 g/L; H ₂ O ₂ 0.68 mg/L; pH 5.0; Temperature 298 K	150 min	79%	[35]
H ₂ O ₂ /Mn-Fe ₂ O ₄	Methylene blue	Natural solar radiation	Catalyst 1.0 g/L; H ₂ O ₂ 2720 mg/L; pH 7.0; Temperature 298 K	80 min	100%	[36]
H ₂ O ₂ /Cu-Fe ₂ O ₄	Methylene blue	Ultraviolet illumination	Catalyst 0.2 g/L; H ₂ O ₂ 0.68 mg/L; pH 5.0; Temperature 298 K	80 min	90%	[37]

3.2.8. Validation of Reclaimed Water

A physicochemical characterization of the water was carried out to determine its potential application. Both dyed wastewater effluents, as well as the water sample treated with the modified Fenton system were characterized. The median values of the wastewater properties, before and after treatment, were determined, and they are listed in Table 6. The performance of the modified Fenton system is clear from the data displayed in Table 6. The results demonstrate that, under UV illumination conditions using the Fenton catalyst, the Chemical Oxygen Demand (COD) reduced from 420 to 38 mg/L. The non-treated dye-containing wastewater presented a high concentration of COD. This resulted from effluent oxidation. Thus, the Fenton reagent treatment was able to oxidize and degrade most of the organics in the wastewater (90% COD removal). Moreover, when compared to the non-treated water, the reclaimed water, that is, the modified-Fenton-treated wastewater, exhibited lower dissolved oxygen (DO), turbidity, and suspended solids. However, the pH declined due to the Fenton reaction being carried out in the acidic range. It is worth mentioning that this acidic range might be altered prior to reuse. Such technology suggests that wastewater might be reused without severe toxicity accumulation. The quality of the dye wastewater treated using the modified Fenton treatment system is good enough for reuse in textile dyeing processes [38–40]. Hence, to verify the possibility of reusing reclaimed water, it is important to perform reuse tests.

Table 6. Wastewater characteristics, including physicochemical properties.

Parameter (Unit)	Suspended Solids (mg/L)	Turbidity (NTU)	pH	DO (mg/L)	COD (mg-COD/L)
Wastewater	120	34	5.0	2.4	420
Treated water	38	2.5	3.0	2.3	28

4. Conclusions

In the current investigation, Levafix dye oxidation as an example of reactive dye molecules in aqueous media was conducted using a modified Fenton technique with Fuller's earth as the elemental catalyst source. SEM and FTIR suggested that the oxidation reaction was highly efficient due to the presence of a porous medium and elemental sources. The Levafix Dark Blue dye removal rates verified the effectiveness of the Fuller's earth-based Fenton treatment system. Response surface methodology based on a Box–Behnken factorial design was used to optimize the operating conditions, and the optimum values were 818 and 1.02 mg/L for Fuller's earth and hydrogen peroxide, respectively. This investigation found that using an optimal pH of 3.0 resulted in a 99% removal rate within 15 min of the illumination time. The kinetic rate equation for the system was best modeled by a second-order equation that well fitted the experimental results. The data of the experimental work, coupled with the calculated thermodynamic parameters, verified the significance of the system in removing azo dye. Therefore, this study demonstrates a sustainable and environmentally benign Fenton system since it is based on a naturally occurring catalyst. It is worth mentioning that the results of the current study have led to the application of such a technique in real textile wastewater effluent. However, more data are required to apply such a system to real textile effluent for both scientists and industrial operators. Additionally, much effort can be made to better design solar photocatalysis to satisfy the industrial sector and operate in a more economic flexible system to meet wastewater treatment requirements. Thus, upgrading such technology could highlight a new opportunity for the industrial sector.

Author Contributions: Conceptualization, M.A.T.; methodology, M.M.N. and M.A.T.; software, H.A.N.; formal analysis, H.A.N.; investigation, M.A.T.; data curation, H.A.N.; writing—original draft, M.M.N. and M.A.T.; writing—review and editing, M.A.T. and H.A.N.; project administration, M.M.N.; funding acquisition, M.M.N. All authors have read and agreed to the published version of the manuscript.

Funding: The authors extend their appreciation to Prince Sattam bin Abdulaziz University for funding this research work through project number (PSAU/2023/01/31544).

Institutional Review Board Statement: Not applicable.

Informed Consent Statement: Not applicable.

Data Availability Statement: Data are available upon request.

Acknowledgments: The authors extend their appreciation to Prince Sattam bin Abdulaziz University for funding this research work.

Conflicts of Interest: The authors declare no conflict of interest.

References

1. Shimi, A.K.; Parvathiraj, C.; Kumari, S.; Dalal, J.; Kumar, V.; Wabaidur, S.M.; Alothman, Z.A. Green synthesis of SrO nanoparticles using leaf extract of *Albizia julibrissin* and its recyclable photocatalytic activity: An eco-friendly approach for treatment of industrial wastewater. *Environ. Sci.* **2022**, *1*, 849–861. [[CrossRef](#)]
2. Uddin, F. Clays, nanoclays, and montmorillonite minerals. *Metall. Mater. Trans. A* **2008**, *39*, 2804–2814. [[CrossRef](#)]
3. Uddin, F. *Montmorillonite: An Introduction to Properties and Utilization*; IntechOpen: London, UK, 2018.
4. Rohilla, S.; Gupta, A.; Kumar, V.; Kumari, S.; Petru, M.; Amor, N.; Noman, M.T.; Dalal, J. Excellent UV-light triggered photocatalytic performance of ZnO. SiO₂ nanocomposite for water pollutant compound methyl orange dye. *Nanomaterials* **2021**, *11*, 2548. [[CrossRef](#)] [[PubMed](#)]
5. Safwat, S.M.; Medhat, M.; Abdel-Halim, H. Phenol adsorption onto kaolin and fuller's earth: A comparative study with bentonite. *Desalination Water Treat.* **2019**, *155*, 197–206. [[CrossRef](#)]
6. Nour, M.; Tony, M.A.; Nabawy, H. Immobilization of magnetic nanoparticles on cellulosic wooden sawdust for competitive Nudrin elimination from environmental waters as a green strategy: Box-Behnken Design optimization. *Int. J. Environ. Res. Public Health* **2022**, *19*, 15397. [[CrossRef](#)]
7. Lv, Q.; Li, G.; Sun, H.; Kong, L.; Lu, H.; Gao, X. Preparation of magnetic core/shell structured γ -Fe₂O₃@Ti-TmSiO₂ and its application for the adsorption and degradation of dyes. *Microporous Mesoporous Mater.* **2014**, *186*, 7–13. [[CrossRef](#)]

8. Su, R.; Chai, L.; Tang, C.; Li, B.; Yang, Z. Comparison of the degradation of molecular and ionic ibuprofen in a UV/H₂O₂ system. *Water Sci. Technol.* **2018**, *77*, 2174–2183. [[CrossRef](#)]
9. Shah, J.; Jan, M.R.; Muhammad, M.; Ara, B.; Fahmeeda. Kinetic and equilibrium profile of the adsorptive removal of Acid Red 17 dye by surfactant-modified fuller's earth. *Water Sci. Technol.* **2017**, *75*, 1410–1420. [[CrossRef](#)]
10. Su, R.; Dai, X.; Wang, H.; Wang, Z.; Li, Z.; Chen, Y.; Luo, Y.; Ouyang, D. Metronidazole degradation by UV and UV/H₂O₂ advanced oxidation processes: Kinetics, mechanisms, and effects of natural water matrices. *Int. J. Environ. Res. Public Health* **2022**, *19*, 12354. [[CrossRef](#)]
11. Wang, Y.; Ye, X.; Chen, G.; Li, D.; Meng, S.; Chen, S. Synthesis of BiPO₄ by Crystallization and Hydroxylation with Boosted Photocatalytic Removal of Organic Pollutants in Air and Water. *J. Hazard. Mater.* **2020**, *399*, 122999. [[CrossRef](#)]
12. Ren, B.; Wang, T.; Qu, G.; Deng, F.; Liang, D.; Yang, W.; Liu, M. In Situ Synthesis of g-C₃N₄/TiO₂ Heterojunction Nanocomposites as a Highly Active Photocatalyst for the Degradation of Orange II under Visible Light Irradiation. *Environ. Sci. Pollut. Res.* **2018**, *25*, 19122–19133. [[CrossRef](#)]
13. Thabet, R.H.; Fouad, M.K.; El Sherbiny, S.A.; Tony, M.A. Identifying optimized conditions for developing dewatered alum sludge based photocatalyst to immobilize a wide range of dye contamination. *Appl. Water Sci.* **2022**, *12*, 210. [[CrossRef](#)]
14. Beltran-Pérez, O.D.; Hormaza-Anaguano, A.; Zuluaga-Diaz, B.; Cardona-Gallo, S.A. Structural modification of regenerated fuller earth and its application, in the adsorption of anionic and cationic dyes. *Dyna* **2015**, *82*, 165–171. [[CrossRef](#)]
15. Nguyen, T.T.; Huynh, K.A.; Padungthon, S.; Pranudta, A.; Amonpattaratkit, P.; Tran, L.B.; Phan, P.T.; Nguyen, N.H. Synthesis of natural flowerlike iron-alum oxide with special interaction of Fe-Si-Al oxides as an effective catalyst for heterogeneous Fenton process. *J. Environ. Chem. Eng.* **2021**, *9*, 105732. [[CrossRef](#)]
16. Mosallanejad, S.; Dlugogorski, B.Z.; Kennedy, E.M.; Stockenhuber, M. On the Chemistry of Iron Oxide Supported on γ -Alumina and Silica Catalysts. *ACS Omega* **2018**, *3*, 5362. [[CrossRef](#)]
17. He, D.; Zhang, C.; Zeng, G.; Yang, Y.; Huang, D.; Wang, L.; Wang, H. A Multifunctional Platform by Controlling of Carbon Nitride in the Core-Shell Structure: From Design to Construction, and Catalysis Applications. *Appl. Catal. B Environ.* **2019**, *258*, 117957. [[CrossRef](#)]
18. Tony, M.A. Valorization of undervalued aluminum-based waterworks sludge waste for the science of The 5 Rs' criteria. *Appl. Water Sci.* **2022**, *12*, 20. [[CrossRef](#)]
19. Wang, Z.; Wang, T.; Wang, Z.; Jin, Y. The adsorption and reaction of a titanate coupling reagent on the surfaces of different nanoparticles in supercritical CO₂. *J. Colloid. Interfac. Sci.* **2006**, *304*, 152. [[CrossRef](#)]
20. Pourali, P.; Behzad, M.; Arfaeina, H.; Ahmadfazeli, A.; Afshin, S.; Poureshgh, Y.; Rashtbari, Y. Removal of acid blue 113 from aqueous solutions using low-cost adsorbent: Adsorption isotherms, thermodynamics, kinetics and regeneration studies. *Sep. Sci. Technol.* **2021**, *18*, 3079. [[CrossRef](#)]
21. Raut-Jadhav, S.; Pinjari, D.V.; Saini, D.R.; Sonawane, S.H.; Pandit, A.B. Intensification of degradation of methomyl (carbamate group pesticide) by using the combination of ultrasonic cavitation and process intensifying additives. *Ultrason. Sonochemistry* **2016**, *31*, 135–142. [[CrossRef](#)]
22. Najjar, W.; Chirchi, L.; Santosb, E.; Ghorhel, A. Kinetic study of 2-nitrophenol photodegradation on Al-pillared montmorillonite doped with copper. *J. Environ. Monit.* **2001**, *3*, 697–701. [[CrossRef](#)] [[PubMed](#)]
23. Guan, S.; Yang, H.; Sun, X.; Xian, T. Preparation and promising application of novel LaFeO₃/BiOBr heterojunction photocatalysts for photocatalytic and photo-Fenton removal of dyes. *Opt. Mater.* **2020**, *100*, 109644. [[CrossRef](#)]
24. Tony, M.A.; Lin, L.S. Performance of acid mine drainage sludge as an innovative catalytic oxidation source for treating vehicle-washing wastewater. *J. Dispers. Sci. Technol.* **2020**, *43*, 50–60. [[CrossRef](#)]
25. Fang, P.; Wang, Z.; Wang, W. Enhanced Photocatalytic Performance of ZnTi-LDHs with Morphology Control. *CrystEngComm* **2019**, *21*, 7025–7031. [[CrossRef](#)]
26. Markandeya; Shukla, S.P.; Dhiman, N.; Mohan, D.; Kisku, G.C.; Roy, S. An efficient removal of disperse dye from wastewater using zeolite synthesized from cenospheres. *J. Hazard. Toxic Radioact. Waste* **2017**, *21*, 04017017. [[CrossRef](#)]
27. Rashed, M.N.; El Taher, M.A.D.; Fadlalla, S.M. Photocatalytic degradation of Rhodamine-B dye using composite prepared from drinking water treatment sludge and nano TiO₂. *Environ. Quality Manag.* **2022**, *31*, 175. [[CrossRef](#)]
28. Elsayed, S.A.; El-Sayed, E.; Tony, M. Impregnated chitin biopolymer with magnetic nanoparticles to immobilize dye from aqueous media as a simple, rapid and efficient composite photocatalyst. *Appl. Water Sci.* **2022**, *12*, 252. [[CrossRef](#)]
29. Nichela, D.A.; Berkovic, A.M.; Costante, M.R.; Juliarena, M.P.; Einschlag, F.S.G. Nitrobenzene degradation in Fenton-like systems using Cu (II) as catalyst. Comparison between Cu (II)- and Fe (III)-based systems. *Chem. Eng. J.* **2013**, *228*, 1148–1157. [[CrossRef](#)]
30. Buthiyappan, A.; Raman, A.A.; Daud, W.M.W. Development of an advanced chemical oxidation wastewater treatment system for the batik industry in Malaysia. *RSC Adv.* **2016**, *6*, 25222. [[CrossRef](#)]
31. Lopez-Lopez, C.; Martín-Pascual, J.; Martínez-Toledo, M.V.; González-López, J.; Hontoria, E.; Poyatos, J.M. Effect of the operative variables on the treatment of wastewater polluted with phthalo blue by H₂O₂/UV process. *Water Air Soil Pollut.* **2013**, *224*, 1725. [[CrossRef](#)]
32. Santana, C.S.; Ramos, M.D.N.; Velloso, C.C.V.; Aguiar, A. Kinetic evaluation of dye decolorization by Fenton processes in the presence of 3-hydroxyanthranilic acid. *Int. J. Environ. Res. Public Health* **2019**, *16*, 1602. [[CrossRef](#)]
33. Feng, J.; Hu, X.; Yue, P.L.; Zhu, H.Y.; Lu, G.Q. Discoloration and mineralization of Reactive Red HE-3B by heterogeneous photo-Fenton reaction. *Water Res.* **2003**, *37*, 3776. [[CrossRef](#)]

34. Parker, H.L.; Budarin, V.L.; Clark, J.H.; Hunt, A.J. Use of Starbon for the Adsorption and Desorption of Phenols. *ACS Sustain. Chem. Eng.* **2013**, *1*, 1311–1318. [[CrossRef](#)]
35. Sum, O.S.; Feng, J.; Hu, X.; Yue, P.L. Pillared laponite clay-based Fe nanocomposites as heterogeneous catalysts for photo-Fenton degradation of acid black. *Chem. Eng. Sci.* **2004**, *59*, 5269.
36. Kalam, A.; Al-Sehemi, A.G.; Assiri, M.; Du, G.; Ahmad, T.; Ahmad, I.; Pannipara, M. Modified solvothermal synthesis of cobalt ferrite (CoFe₂O₄) magnetic nanoparticles photocatalysts for degradation of methylene blue with H₂O₂/visible light. *Results Phys.* **2018**, *8*, 1046–1053. [[CrossRef](#)]
37. Desai, H.B.; Hathiya, L.; Joshi, H.; Tanna, A. Synthesis and characterization of photocatalytic MnFe₂O₄ nanoparticles. *Mater. Today Proc.* **2020**, *21*, 1905–1910. [[CrossRef](#)]
38. Guo, X.; Wang, K.; Xu, Y. Tartaric acid enhanced CuFe₂O₄-catalyzed heterogeneous photo-Fenton-like degradation of methylene blue. *Mater. Sci. Eng.* **2019**, *245*, 75. [[CrossRef](#)]
39. Meghwal, K.; Agrawal, R.; Kumawat, S.; Jangid, N.K.; Ameta, C. Chemical and Biological Treatment of Dyes. In *Impact of Textile Dyes on Public Health and the Environment*; IGI Global: Hershey, PA, USA, 2020. [[CrossRef](#)]
40. Meghwal, K.; Kumawat, S.; Ameta, C.; Jangid, N.K. Effect of dyes on water chemistry, soil quality, and biological properties of water. In *Impact of Textile Dyes on Public Health and the Environment*; IGI Global: Hershey, PA, USA, 2020; pp. 90–114. [[CrossRef](#)]

Disclaimer/Publisher's Note: The statements, opinions and data contained in all publications are solely those of the individual author(s) and contributor(s) and not of MDPI and/or the editor(s). MDPI and/or the editor(s) disclaim responsibility for any injury to people or property resulting from any ideas, methods, instructions or products referred to in the content.